International Institute for
Applied Systems Analysis
Schlossplatz 1
A-2361 Laxenburg, Austria

Tel: +43 2236 807 342
Fax: +43 2236 71313
E-mail: publications@iiasa.ac.at
Web: www.iiasa.ac.at

Interim Report **IR-12-005**

Changes in the onset of spring and uncertainty in 21st century terrestrial carbon sinks

Carl Salk (carlsalk@gmail.com)

Approved by

Michael Obersteiner
Program Leader, Ecosystems Services and Management

April 23, 2012

International Institute for Applied Systems Analysis
Registration number: ZVR 524808900

Contents

Abstract

A growing imperative in climate change research is to understand the relative carbon balance of terrestrial ecosystems when they are perturbed by warming and other climate changes. A key limit on potential carbon fixation by deciduous forests is growing season length, a variable know to be sensitive to temperature. Models are a tempting method to untangle species' budburst cues and forecast phenology under warmer climate scenarios. I tested two models' ability to recover parameters used to simulate budburst data. The simpler model was cued only by spring warmth while the complex one modulated warmth requirements with chilling exposure. For the simple model, parameters could be recovered consistently from some, but not all, regions of parameter space. The complex model's parameters were largely unrecoverable. To understand the consequences of parameter uncertainty, I applied both models to an 18 year phenological record of 13 deciduous tree species. While a few species fell into identifiable regions of the simple model's parameter space, most did not, and projected budburst dates had wide parameter-derived uncertainty intervals. These bands were wider still under a 5°C warming scenario. Even greater uncertainty resulted from the complex model. These results suggest that attempts to forecast the timing trees' growing seasons, and therefore their potential for carbon fixation in warmer climates, should be treated with caution.

Acknowledgments

The author would like to thank Carol Augspurger for sharing the phenological data that she has meticulously collected for the past 20 years. In addition, thanks are due to James S. Clark and Alan Gelfand for their advice on early stages of this work and Matthias Jonas who supervised the later stages during the Young Scientists Summer Program of 2010. Additional support was provided by a Graduate Research Fellowship from the US National Science Foundation.

About the Authors

Carl Salk took part in the Young Scientists Summer Program at IIASA during 2010 where he did this work. He has since completed his PhD at Duke University, and will begin a postdoc at the University of Colorado, Boulder, in January 2012.

Changes in the onset of spring and uncertainty in 21st century terrestrial carbon sinks

Carl Salk

1. Introduction

Recent attempts to regulate atmospheric greenhouse gases give new urgency to understanding their sources and sinks (IPCC, 2007). Fixed carbon is stored in many different pools in terrestrial ecosystems, from soil organic matter to tree trunks. These pools are ultimately fed by a single process: photosynthesis. Because they store so much carbon per unit area, forests play a key role in atmospheric greenhouse gas balance; understanding the function of trees in the face of climate change is crucial. Calculations by the Global Carbon Project based on global vegetation models estimate that 29% of anthropogenic CO_2 emissions from fossil fuels and land use change are removed from the atmosphere by terrestrial vegetation (LeQuéré et al., 2009). While terrestrial sequestration is an opportunity for carbon budget management in countries with extensive forests, such schemes must account for uncertainties in forest carbon fluxes to contain the risk of overshooting emissions targets (Lieberman et al., 2007). Terrestrial carbon accounting projections are complicated because forest carbon balance may not follow historical patterns under an altered climate. This is caused by climate-sensitive processes ranging from tree physiology to stand-replacing wildfires (Galik and Jackson, 2009). Understanding the balance of these factors is central to projecting the forests' utility in carbon sequestration.

This report addresses direct climate impacts on one source of uncertainty in terrestrial carbon balance: growing season length. The amount of time during a year that is available for photosynthesis is directly determined by the timing of leaf growth and senescence, also known as 'phenology' (Jolly et al., 2005). While spring and fall phenology are equally important in terms of growing season length, they are not equal in their effect on carbon fixation. In this respect, spring phenology is more important, and is the focus of this report. Spring leaf growth happens closer to the summer solstice (when more light is available) than does autumn leaf drop (Harrington et al., 1989). In addition, young leaves have a higher capacity for photosynthesis than old, degraded leaves (Augspurger et al., 2005).

Interannual variability of budburst timing is a source of trees' resilience to climate change, and could provide a dampening feedback to increasing atmospheric CO_2 (Peñuelas et al., 2009). Analyses of phenological records from the last 30 years show a

trend toward earlier spring events (Parmesan and Yohe, 2003; Menzel et al., 2006). Observations of earlier budburst are consistent with a response to late 20th century warming, but extrapolation of such trends does not provide a robust basis for projections of future changes.

Models based on underlying plant physiology are the best way to make plausible projections of future budburst dates (Morin et al., 2007). Experiments have demonstrated that tree species do not necessarily have a linear relationship to warmer temperatures and shifts in budburst dates (Myking, 1997). Many species have a safety mechanism that can only be unlatched by sufficient chilling exposure (Sarvas, 1974). This prevents early budburst during winter warm spells. A chilling requirement has been included in many prognostic models of budburst timing that have been parameterized with multi-year observational datasets (e.g. Cannell and Smith, 1983; Chuine, 2000). These models continue to be used to forecast shifts in trees' leafing dates under climate change (e.g. Morin et al. 2008; Harrington et al. 2010), and have been used as inputs for projections of changes in carbon budgets (e.g. Picard et al., 2005) or tree species distribution (e.g. Morin et al., 2007). However, uncertainty in projected leafing dates is rarely if ever estimated. Differences among these budburst models have substantive consequences for climate change projections. A basic model that includes only spring warmth has only one possible response to increasing temperatures: earlier budburst. However, models that include chilling can exhibit a range of complexity, even to the extent of later budburst with warming if chilling requirements are not met (Morin et al., 2008).

A less obvious problem with phenological projections is uncertainty in parameter estimates (Magliavacci et al., 2008). Phenological models necessarily use many parameters. Such models may not be useful if their parameters cannot be identified. If there are multiple combinations of parameters that give a similar fit to data, an extrapolation to future climate using a single set of parameters could be misleading. Even if a model correctly reflects the biological process of budburst, it may not be possible to precisely estimate parameters because of insufficient length and year-to-year variability of phenological datasets. Thus, a model may be biologically robust, but data limitations prevent it from revealing the underlying biology of tree phenology. However, reliable phenological projections could still be possible as long as the different sets of parameters give similar projections of budburst dates.

Phenological responses to identical cues differ widely among species (Howard, 1910), so tree species are likely to show dissimilar responses to climate change. Because it is unfeasible to individually evaluate all temperate tree species, finding patterns shared within evolutionarily or functionally related groups would broaden the impact of phenological studies. This study examines budburst timing sensitivity in two physiologically contrasting tree types: those with ring-porous and diffuse-porous wood. These two wood types differ in xylem diameter. Diffuse-porous species have narrow xylem, which conducts water inefficiently, but is less prone to disfunction, while ring-porous species have wide and hydraulically efficient, but frost-sensitive, xylem (Tyree and Zimmerman, 2002). This has implications for potential frost damage if spring development begins too early.

In this report, I investigate the uncertainties in phenological forecasts, including the overlooked problem of parameter uncertainty. Rather than selecting a single set of

optimal parameters as is typical for such studies, a realistic accounting for uncertainty is provided by estimating parameters' probability distributions. This is done by simulating budburst data with known parameters and real weather data under two models of different complexity from the phenological literature. Estimation of the parameters is then attempted to gain a sense of what level of budburst date uncertainty exists in different parts of parameter space. The same process of parameter estimation is then applied to 13 tree species native to the Midwestern USA. This gives us the strongest possible context for interpreting species' parameter distributions and budburst date uncertainties under climate change.

The goal of this research is to address several questions:

1) How recoverable are parameters under two commonly used phenological models?

2) How are budburst dates likely to change in a warmer climate?

3) How much uncertainty is there in such projections?

4) Are species with different wood anatomies likely to respond differently to warmer temperatures?

2. Methods

2.1 Weather Data

The weather datasets used in this study are maintained by the Illinois State Water Survey. All weather data used in this study came from the station nearest to the study site, about 8 km to the southwest, in Champaign, IL. The station is on the edge of the University of Illinois agricultural experiment fields, just south of the main campus. Daily mean temperatures from 1992-2010 were used in fitting parameters for phenological models. The same data for 1901-1991 were used to generate budburst projections under different climate scenarios.

2.2 Phenological Data

The phenological observations were made by Carol Augspurger during the spring of 18 years, from 1993-2010. Observations were made in Trelease Woods, a ~24 ha forest fragment about 5 km northeast of Urbana, IL. All observations are made on permanently tagged trees, ensuring that the same individuals were observed each year. The date of budburst was defined as the first day on which leaf tissue was visible emerging from at least 1/3 of a tree's buds. Observations were made at ~7 day intervals. Dates for all trees in a given species were averaged to obtain a population-level phenological date and help overcome the limitation of relatively wide observation intervals. Further details are found in Augspurger and Bartlett (2003).

2.3 Phenological Models

There are many published models that generate projected budburst dates when supplied with weather data and appropriate parameters. These parameters presumably reflect the

underlying physiology of a tree or species, but in practice they are not currently derivable from first biological principles. In all models, warmth promotes budburst, an effect that is supported by multiple forms of evidence. The simplest model requires only warmth to trigger leaf growth. This basic relationship has been understood for over 250 years (Réaumur, 1735). In its modern sense, this is sometimes called the 'spring warming' (hereafter SW) model (Hunter and Lechowicz, 1992). Some species have mechanisms to prevent premature leaf growth during brief winter warm spells. While these mechanisms are poorly understood, greenhouse and observational studies suggest that over-winter chilling exposure makes many species more receptive to warmth in spring. To incorporate this effect, models include a tradeoff between chilling and warmth. For the purpose of this report I focus on the chilling-forcing (hereafter CF) model of Cannell and Smith (1983) because its mathematical structure was presented in an easy to interpret way. All abbreviations used in this section are summarized and defined in Table A1, and the parameters of both models are summarized in Table A2.

A degree-day sum is at the center of both types of models. The degree-day sum (DD) is a non-decreasing function of date, calculated from average daily temperatures with parameters of starting date (*startdate*) and threshold temperature (*thresh*):

$DD_y(t) = \sum_{d=startdate}^{t} (T_{d,y} - thresh) I_{d,y}$ where $I_{d,y}=1$ if $T_{d,y}>thresh$ and $I_{d,y}=0$ otherwise. In this formula, t is the Julian calendar date, y is the year and $T_{d,y}$ is the daily average temperature.

Within the SW model, the expected date of budburst (*BBE*) is the first date satisfying:

$BBE_y = t^*$ such that $DD_y(t^*) > DD^*$

The optimum value of DD^* is a trivial function of the two other parameters and is calculated rather than estimated as a parameter. The value of DD^* is invariant across years. Thus there are a total of three parameters to estimate under this model, *startdate, thresh*, and σ, the variance on the error term from the model assessment phase (see section 2.2.4 below).

The CF model uses the same degree-day calculation, but has a critical sum that decreases as a function of accumulated chilling:

$DD^*(t) = ff + gg \cdot \exp(-hh \cdot CD(t))$

where *ff, gg* and *hh* are parameters. $CD(t)$ is the accumulated number of chill days (CD) to day t:

$CD_y(t) = \sum_{d=1\,sept}^{t} L_{d,y}$ where $L_{d,y}=1$ if $T_d<ct$ and $L_{d,y}=0$ otherwise.

This adds another parameter, the chilling threshold (*ct*). Following Cannell and Smith (1983), the starting date for degree-days was set to February 1, and for chilling days to September 1 in the previous fall. This leaves a total of six parameters: *thresh*, *ff*, *gg*, *hh*, *ct*, and σ.

2.4 Model Assessment

To assess the mathematical robustness of phenological models, I generated simulated data from known parameters. Simulations were generated over the same years and same weather data as were used in the recovery of parameters from observations of actual trees. I then attempted to recover the parameter values used in simulation using a Bayesian model. This technique uses Bayes' Theorem to find probabilities of parameter values given data. This is an advantage over likelihood-only approaches which only allow computation of probabilities of data given parameters.

Central to the Bayesian framework is the likelihood, used to assess both phenological models, which is a simple relationship between observed and predicted budburst dates:

$$BBO^y - BBE^y \sim N(0,\sigma)$$

where BBO_y is the observational data (date of budburst in year y), and BBE_y is the expected budburst date, a function of the weather in year y and the parameters of the specific model in use. The parameter σ is the variance on a normally distributed error term with a mean of zero. This relationship can be used to assess any model that generates predicted budburst dates.

Bayesian calculations require prior distributions for parameter probabilities. In this case, I used uninformative (flat) priors:

$p(\sigma) = \text{IG}(\alpha=.1, \beta=1)$

$p(thresh) = p(ct) = \text{Unif}(-\infty,\infty)$

$p(startdate) = \text{Unif}(\text{September } 1^{st} \text{ of the previous year}, \infty)$

$p(ff) = p(gg) = p(hh) = \text{Unif}(0, \infty)$

In cases where these priors have limits, the limits are to keep parameters within reasonable bounds. For the SW model, the parameter *startdate* wasn't allowed to precede September 1 of the previous year and *thresh* was unbounded. In the CF model, the parameters *f, g* and *h* were constrained to be positive. For both the SW and CF models, the error term variance (σ) was modeled with a weak inverse gamma prior. This put a lower bound of zero on the variance, and allowed for efficient computation of its posterior probability distribution via Gibbs sampling. In this case, the improper (unbounded on at least one end) priors are not a problem because the variance has a proper prior. To estimate the (unknown) distributions of the parameters, I used the Metropolis algorithm (Metropolis et al., 1953) to sequentially sample the parameters' posterior distributions. This is known as Markov-chain Monte Carlo (MCMC) sampling. Details of this process can be found in Clark (2006).

Two-hundred sets of simulated budburst dates were generated from randomly chosen parameters and the weather data set from Champaign Illinois for both model types. These simulated data sets were 18 years long, from 1993 to 2010, the same duration as the Augspurger phenological data. The parameters were selected so that simulated budburst dates were usually between mid-April and mid-May, as is typical for most deciduous species during normal weather years in Central Illinois.

Parameters for simulation were chosen at random for each run. Each run was initialized with a second set of randomly drawn parameters. It was run for 20,000 steps. The first

10,000 were discarded as burn-in. Visual inspection of the resulting chains showed this to be a sufficient burn-in period. All but every 10^{th} of the remaining steps were discarded to reduce autocorrelation and computational burdens. The remaining 1000 steps were used for all subsequent analyses.

To assess these models for parameter recoverability the root-mean-square (RMS) error was calculated between the underlying parameter values used in simulation, and the elements of the thinned chain. This calculation reflects both the accuracy and precision of parameter recovery.

To assess the effects of parameter uncertainty on projections of leafing behavior under climate change, budburst dates were simulated for the 90 years from 1902-1991, years' whose data was not used in model parameterization. This process was repeated for all 1000 sets of retained parameters. The 95% central interval of these dates was computed as a measure of uncertainty in budburst dates under a particular model run. As a simple climate change scenario, 5°C was added to all temperature observations in the 1902-1991 weather dataset. The value of 5°C was chosen as a warm but not extreme climate scenario based on the projections in the latest IPCC report (2007). The procedure of budburst forecasts and credible interval calculations was repeated for this warmer scenario. Also calculated was the mean temperature during the two weeks following budburst. This was used as a measure of trees' ability to phenologically track warmer temperatures, and maximize use of the period of growth permitting temperatures.

2.5 Parameterization of models from observational budburst data

To understand the consequences of parameter uncertainty on climate feedbacks, it is necessary to understand how native tree populations will react to warmer temperatures. To do this I used the MCMC sampling techniques described above to compute probabilities densities of budburst dates under different climate scenarios for 13 canopy tree species native to central Illinois, USA under the SW and CF models. Details of these species are listed in Table 1.

The MCMC routine was run similarly to the simulations for each combination of species and model. To avoid initiation bias, each run began with a randomly drawn set of parameters.

Table 1. List of study species and their wood anatomy. Family classifications follow Stevens (2001 onwards). Wood anatomy classifications follow Perkey et al. (1994).

Species	Family	Wood anatomy
Acer saccharum	Sapindaceae	Diffuse porous
Aesculus glabra	Sapindaceae	Diffuse porous
Carya cordiformis	Juglandaceae	Ring porous
Carya ovata	Juglandaceae	Ring porous
Celtis occidentalis	Cannabaceae	Ring porous
Fraxinus americana	Oleaceae	Ring porous

Gymnocladus dioicus	Fabaceae	Ring porous
Juglans nigra	Juglandaceae	Ring porous
Quercus macrocarpa	Fagaceae	Ring porous
Quercus rubra	Fagaceae	Ring porous
Tilia americana	Malvaceae	Diffuse porous
Ulmus americana	Ulmaceae	Ring porous
Ulmus rubra	Ulmaceae	Ring porous

3. Results

3.1 Simulated Data: Parameter Recovery and budburst Projections

3.1.1 Spring Warming Model

3.1.1.1 Parameter Identifiability and fit of Projections

The recoverability of parameters from data simulated under the SW model varied greatly among runs as a function of the parameters' values (Figure 1). The following paragraphs report mean RMS error between parameters used for simulation of budburst dates and the posterior distributions of these parameters. For brevity, this is referred to as 'RMS error'.

The RMS error for the parameter *thresh* had a median value of 3.08 °C across all runs, with a range from .591 to 319 °C. This median is smaller than the range over which simulated parameters were drawn (0-10 °C), indicating differences among simulations were at least minimally detectable. However, in some cases, RMS error exploded to huge values. While data constrained *thresh* from becoming unreasonably high, no such constraint existed for low values; the MCMC algorithm sometimes wandered into a very low temperature range for *thresh*, leading to large RMS errors for that parameter.

The *startdate* parameter was also recoverable under some circumstances with median error of 32.4 days (range 1.29 to 114). While an error of a month is clearly inaccurate, it is still smaller than the 120 day range (1 December – 31 March) over which simulation parameters were drawn.

The variance (parameter σ) had a median RMS error of 15.3 days^2 (range 1.82 to 102 days^2). The median value is smaller than the range of parameter simulation (between 4 and 64 days^2), indicating some useful recoverability. However, in 22% of simulations, RMS error of σ exceeded the value of that parameter, indicating poor recovery.

While the low end of these ranges indicates that all parameters were precisely estimated in some runs, the high end values indicate that no parameter is universally recoverable under this model.

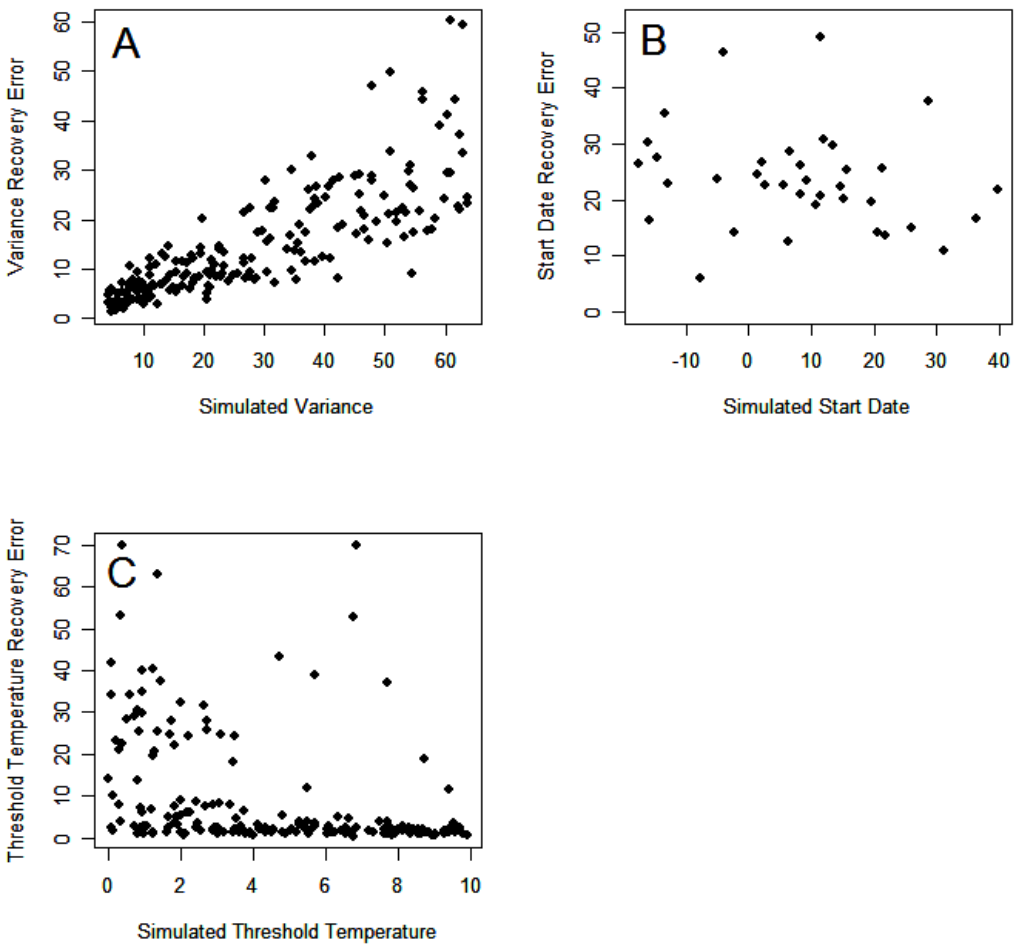

Figure 1. The relative difficulty of recovering parameters from data simulated under the SW model under various circumstances. 1A: RMS error of variance recovery as a function of variance parameter used in simulations. Variance parameter values are generally most recoverable when this parameter's value is small. 1B: Start date recovery error when simulated start date is in mid-winter (range shown equivalent to 10 Dec – 10 February) and threshold temperature is between 5 and 10°C. Under these circumstances, startdate recovery is never particularly good. 1C: Recovery of parameter thresh typically becomes easier as it takes on larger values.

Some parts of parameter space lend themselves to easier recovery than others. Generally speaking, when the simulated value of *thresh* was lower than 5° C it became much harder to recover than when it was higher (Figure 1c). This was particularly true when the error term variance (σ) was high. *Startdate* was difficult to recover as well. In many cases when *thresh* was well identified, *startdate* remained difficult to determine (Figure 2). Identifiability of *startdate* improved slightly when later values were used in simulation.

RMS error between observed and predicted budburst dates ranged from 1.70 to 11.6 days. There was no detectable relationship between either *thresh* or *startdate*, but increasing σ led to a higher RMS error (Figure 3).

3.1.1.2 Climate Change Projections

Within the SW model, sensitivity of budburst to warming depends on model parameters. The parameter *startdate* drives most of this pattern, with later starting dates allowing less advancement of budburst under warmer temperatures (Figure 4). Depending on parameters, sensitivity to 5°C climate change ranged from 2.0 days to 48 days.

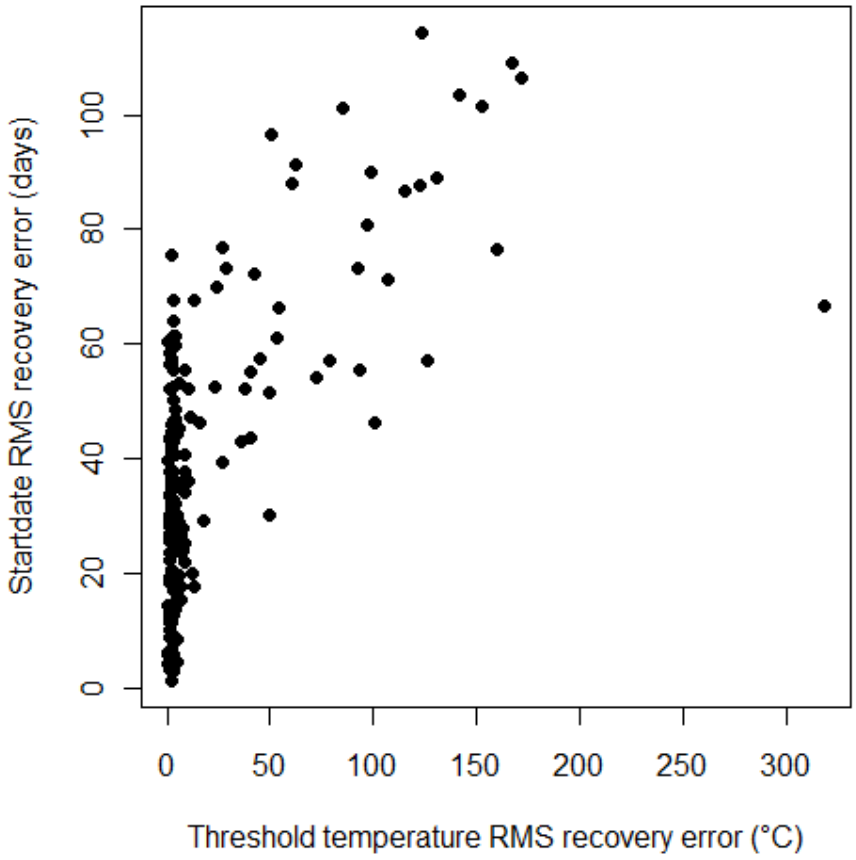

Figure 2. The relationship between recovery of the thresh and startdate parameters under the SW model. Even when *startdate* was difficult to recover (high error values), it was possible to recover *thresh* under some circumstances.

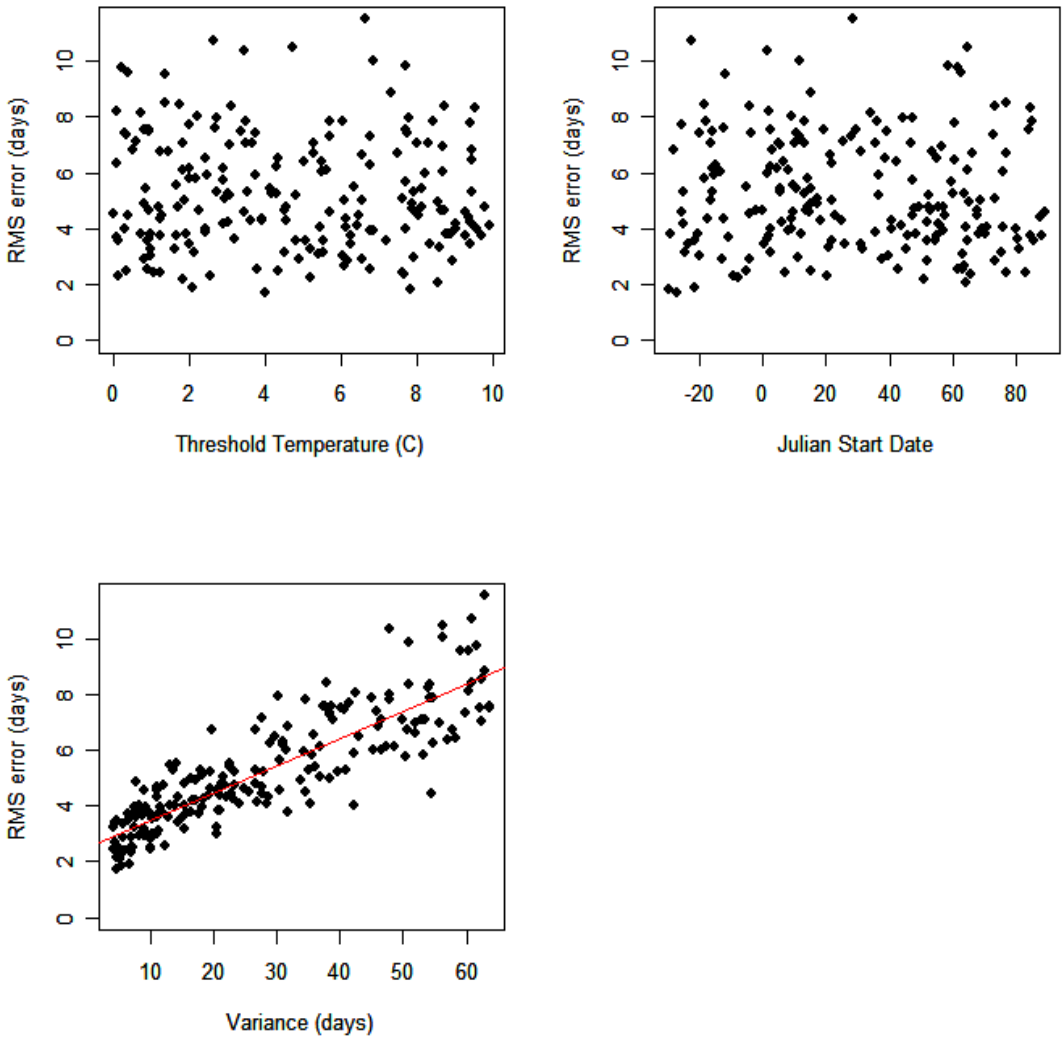

Figure 3. Predictive error between observed and predicted budburst dates as a function of parameters used in data simulation. Fit for variance: R^2=.74, p<.001.

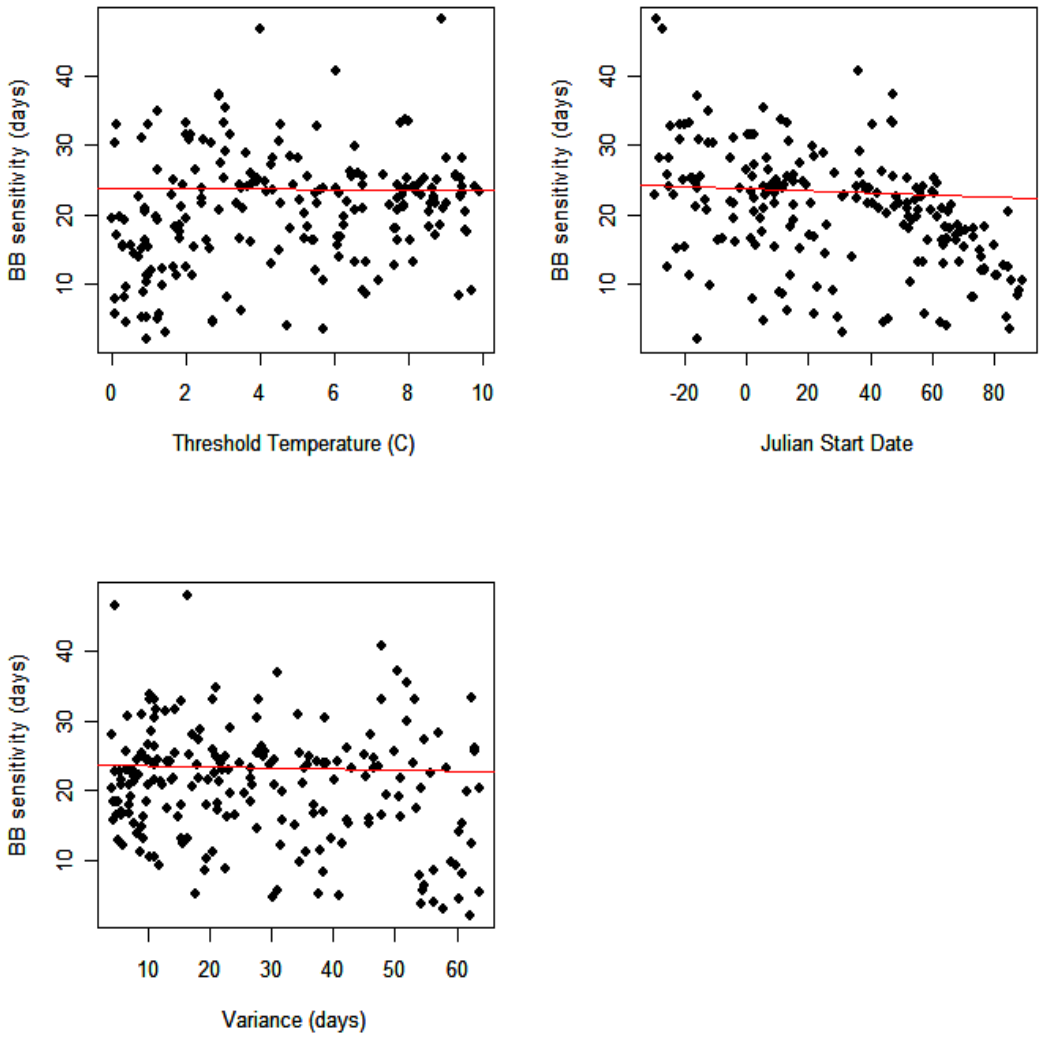

Figure 4. Advancement in days of budburst date due to 5°C warming above 20th century conditions as a function of different parameter values under the SW model. Lines show correlations with p<.05. However, all R^2 values were below .03.

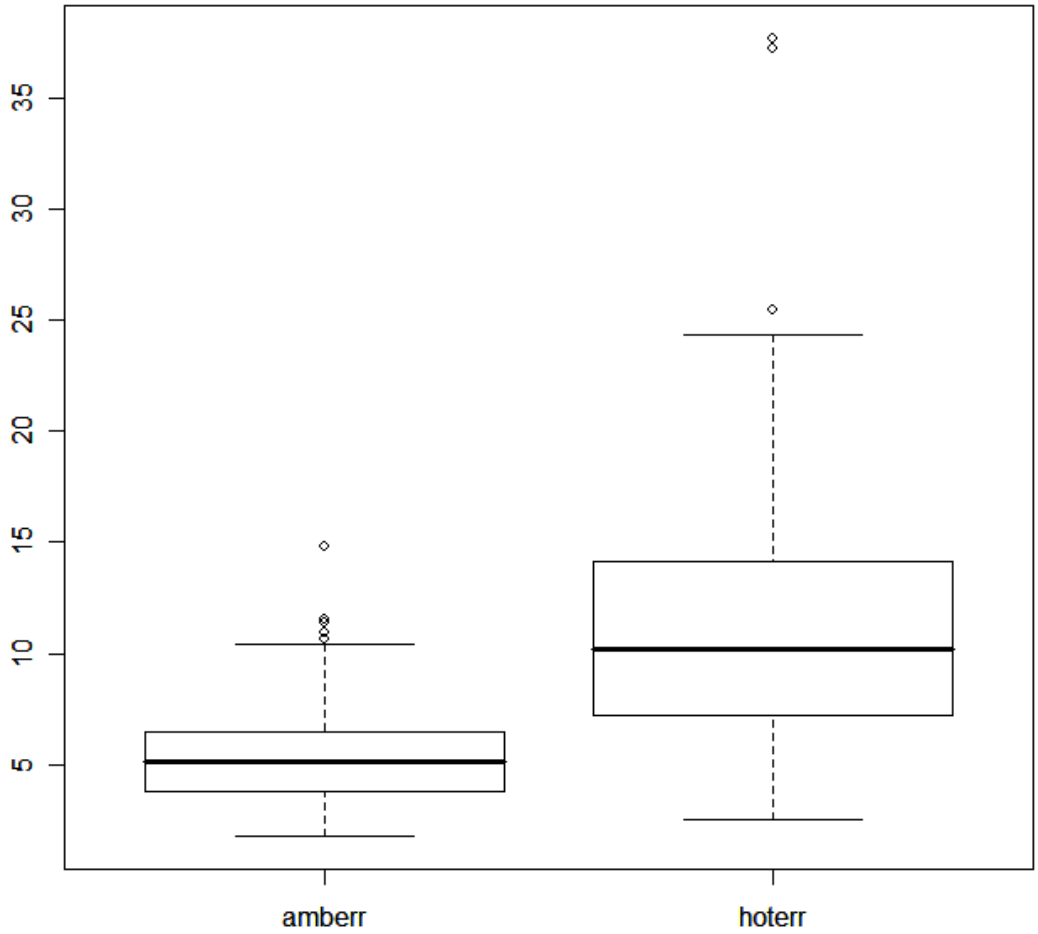

Figure 5. The width in days of the 95% central range of projected budburst dates from simulated data under the SW model. "Amberr" refers to dates projected under 20th century temperatures, while "hoterr" refers to error in projected dates with 5°C added to the same temperature data.

Parameter uncertainty caused variability in projected budburst dates on the 1902-1991 temperature dataset. At 20th century temperatures, the mean within-year 95% central range of budburst dates due to parameter uncertainty was 5.4 days. With temperatures 5°C hotter than the 20th century, mean projected budburst date uncertainty increased to 11.0 days (Figure 5).

3.1.2 Chilling-Forcing model

3.1.2.1 Parameter Identifiability and Fit of Projections

Parameter recoverability from data simulated with the CF model was generally difficult. Most parameters had a median RMS error somewhat smaller than the scale over which they are generated, indicating some slight hope of useful parameter recovery. All parameters had instances of low RMS error. However, for all parameters except σ,

RMS error sometimes exceeded the range over which simulation parameters were drawn by an order of magnitude (Table 2).

Table 2. Quantiles of parameter recovery error using simulated data for the six parameters of the CF model.

	Parameter					
Quantile	*thresh*	*ct*	*ff*	*gg*	*hh*	σ
0	.392	.0945	15.5	114	.00117	1.37
.025	.673	.395	20.0	715	.00202	2.67
.5	2.06	14.5	78.3	2250	.0635	27.0
.975	23.5	39.5	292	5260	.179	68.2
1	40.9	56.1	363	5850	.253	81.4

Unlike the SW model, few clear patterns of parameter identifiability were seen (Figure 6). However, due to the computational difficulties of a six dimensional parameter space, it is possible that patterns exist that simply weren't uncovered. As with the SW model, there was a clear trend toward higher RMS error in all parameters with increasing σ (Figure 6).

RMS error of observed vs. predicted budburst dates was similar to the scale found in the SW model, ranging from 1.66 to 13.9 days. As under the SW model, there was no relationship between any parameter and predictive error except for the σ term (Figure 7).

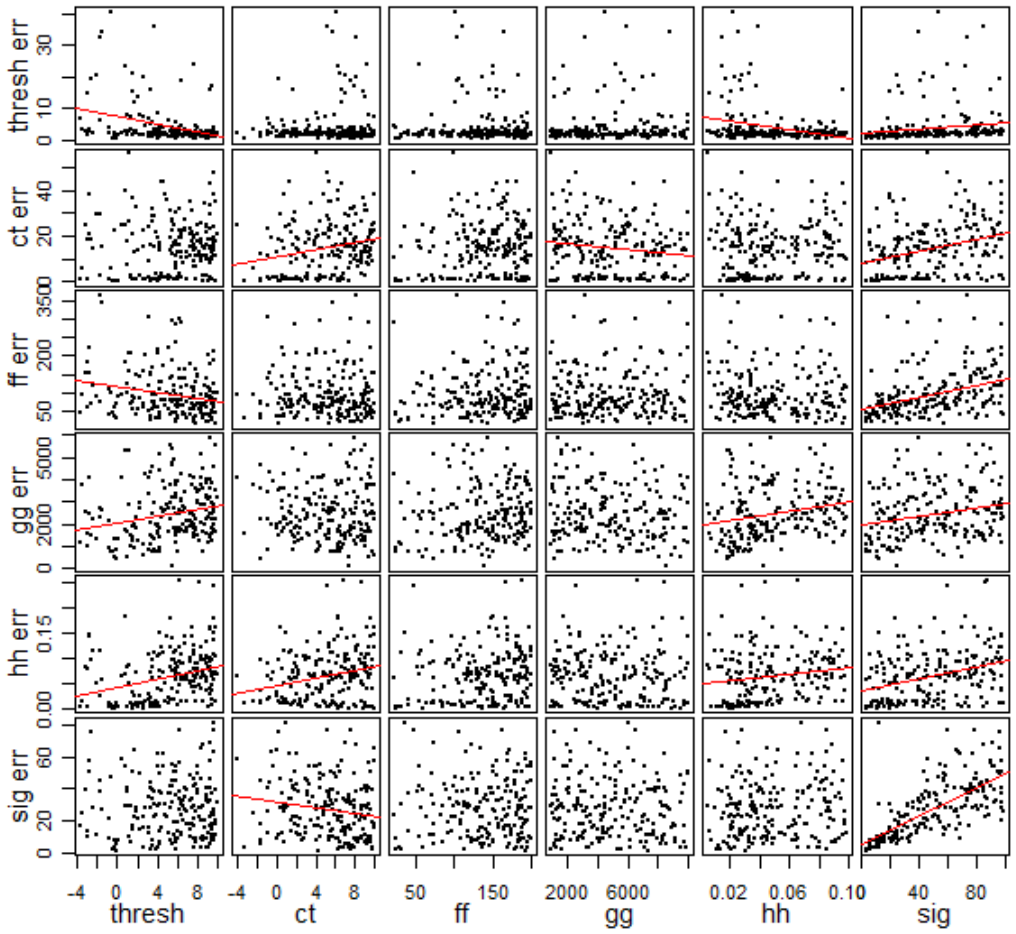

Figure 6. All parameters used in simulation of data under the CF model (x-axes) plotted against recovery errors of all parameters. Lines indicate correlations with p<.05.

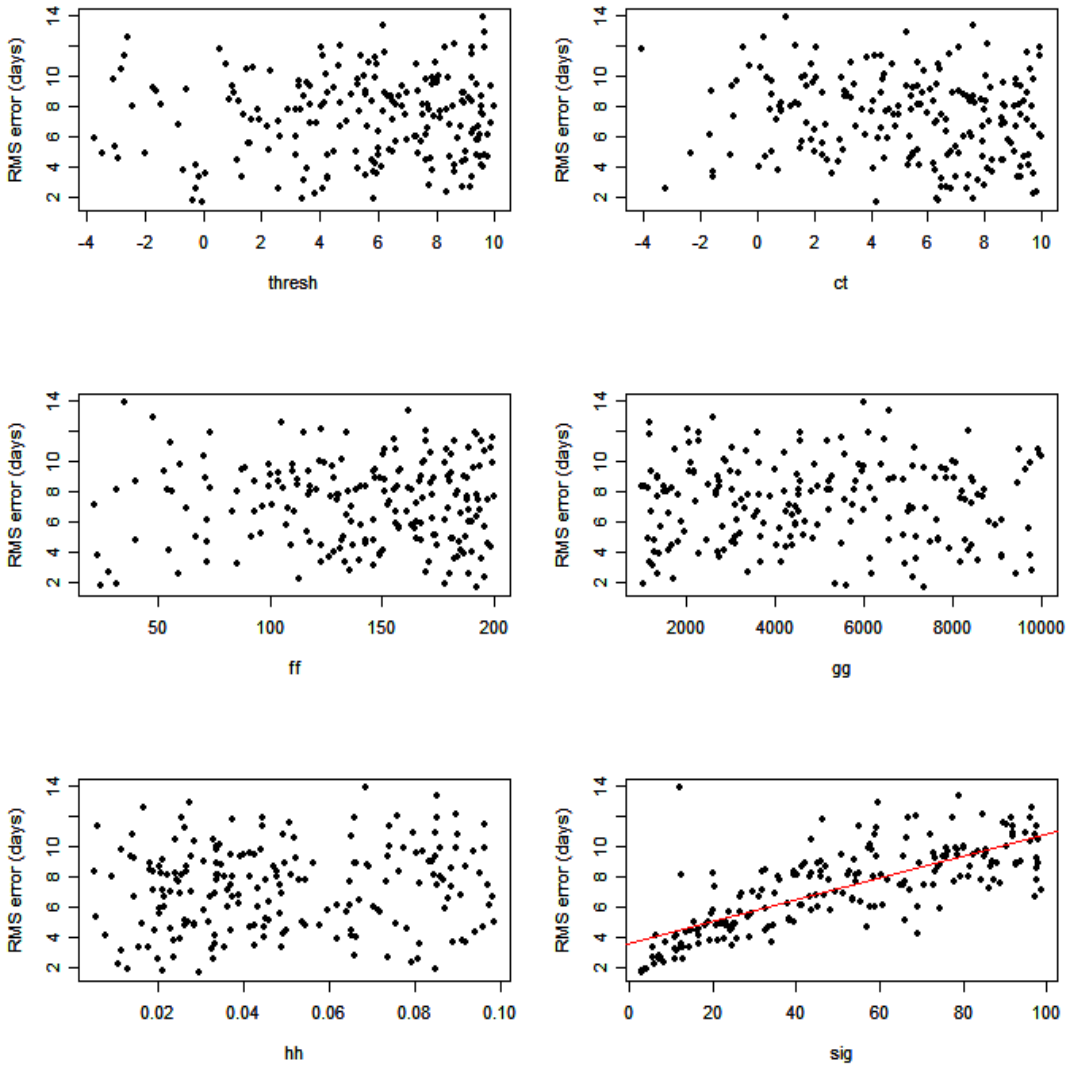

Figure 7. The relationship between parameters used to simulate data under the CF model and RMS error of budburst predictions. The line for the variance term represents a significant correlation with p<.001 and R^2=.57.

3.1.2.2 Climate Change Projections

Under the CF model, projected sensitivity to 5° C warming varied wildly as a function of parameter values. Warming effects on budburst date ranged from a 56 day advancement, to a 25 day delay (Figure 8). A delay in budburst date due to warming is possible under this model because less chilling exposure leads to greater degree-day requirements. The upper limit of about 25 days advance of budburst date shown in Figure 8 is an artifact of the model. A starting date of 1 February for degree-day calculations was used in this model in accordance with the model of Cannell and Smith (1983); see methods section. However, as found for the SW model, maximum possible

budburst advancement due to warmer temperatures is strongly tied to the starting date for counting degree-days (see Figure 4).

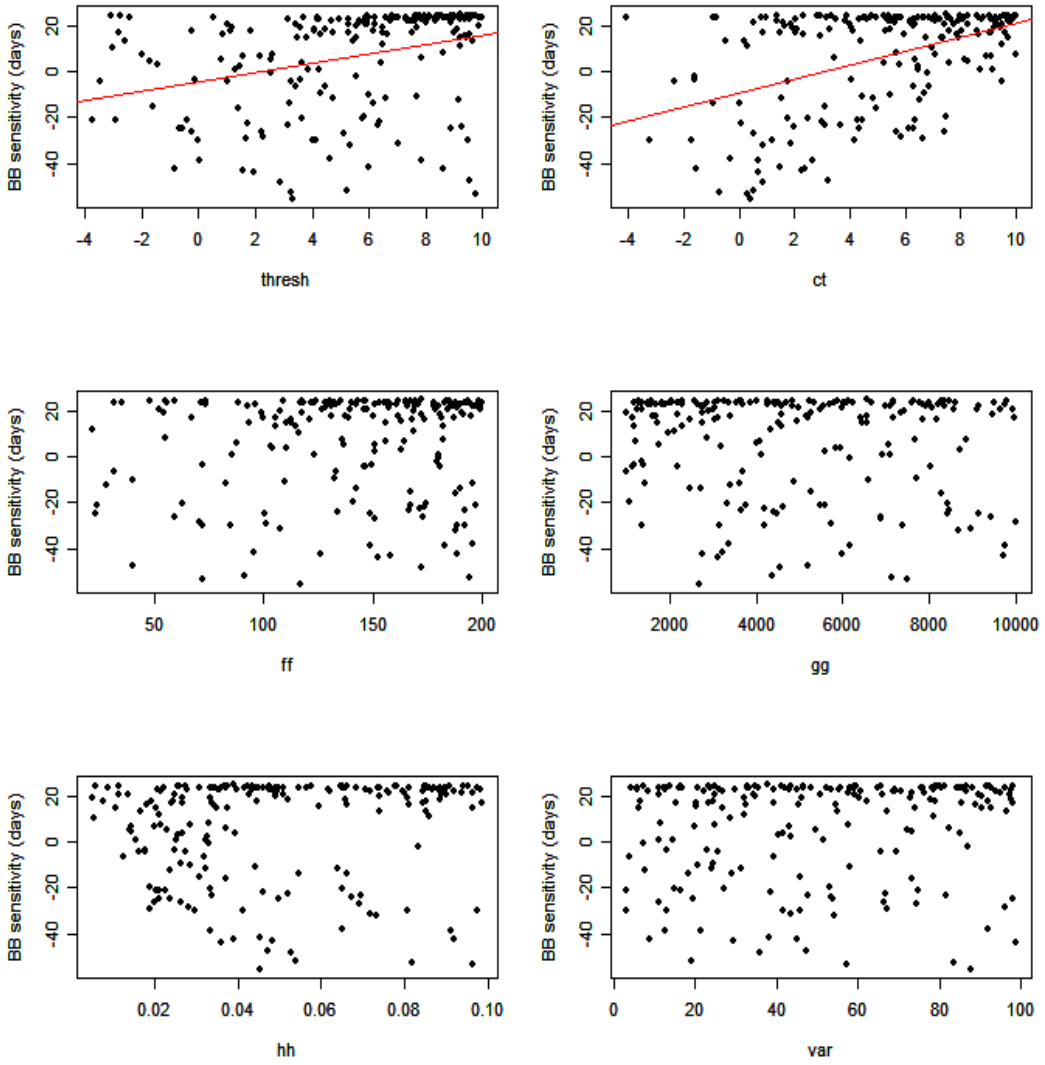

Figure 8. Sensitivity of budburst date to 5°C warming above 20th century conditions as a function of parameter under the CF model. Lines indicate correlations with p<.05.

Uncertainty in parameter recovery led to a substantial increase in projected budburst date uncertainty. Under 1902-1991 temperatures, the mean within-year 95% central range of budburst dates was 9.4 days. When 5°C was added to this temperature dataset, this budburst date uncertainty increased to 30.3 days (Figure 9).

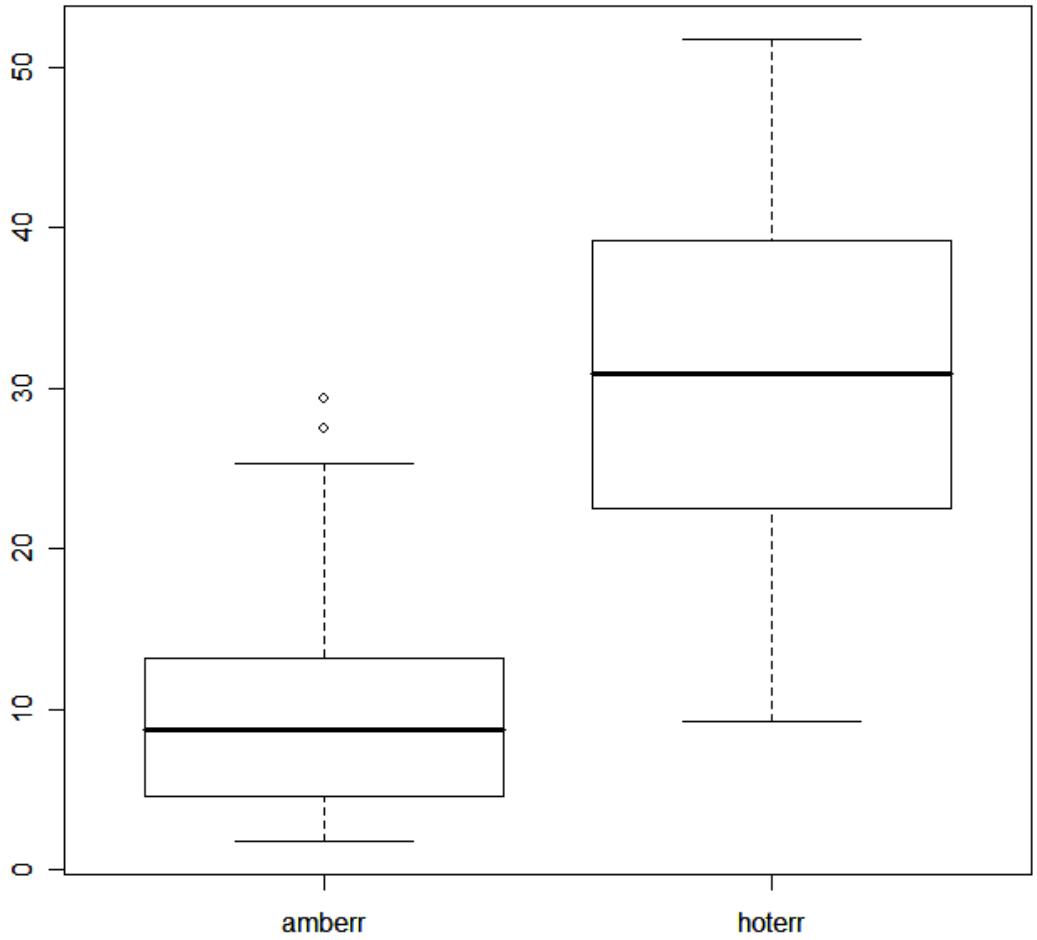

Figure 9: The width in days of the 95% central range of projected budburst dates from simulated data under the CF model. "Amberr" refers to dates projected under 20th century temperatures, while "hoterr" refers to error in projected dates with 5°C added to the same temperature data.

3.2 Parameter Identifiability and Budburst Projections from Observational Data

3.2.1 Spring Warming model

Under the SW model, the identifiability of parameters varied widely among species. The 95% credible interval (CI) for the posterior distribution of the parameter *thresh* was generally wide, from a minimum of 3.9 °C for *Quercus macrocarpa* to a maximum of 168.6 °C for *Carya ovata* (Figure 10). About half of the species had median values of *thresh* within the physiologically plausible range (above 0°C). These species also had the narrowest CIs. The remaining species had very low and wide CIs for *thresh*. Extremely low values of *thresh* indicate that this parameter is measures time

passed, rather than total temperature exposure, suggesting that simple thermal time sum alone is not a realistic model of how these species determine budburst dates.

For the *startdate* parameter, the posterior CI width ranged from 5 d for *Gymnocladus dioicus* to 220 d for *Ulmus rubra*, with most species having wide intervals. The three species with well identified values of *startdate* also had values of *thresh* in the realistic range (Figure 10). However, some species with well identified *thresh* values had *startdate* estimates that covered the entire winter period when temperatures are consistently below the value of *thresh*. As with the findings from simulations, the *startdate* parameter is unrecoverable under these conditions. The variance parameter was generally better behaved, and had a smaller and narrower CI when one or both of the other parameters were well identified.

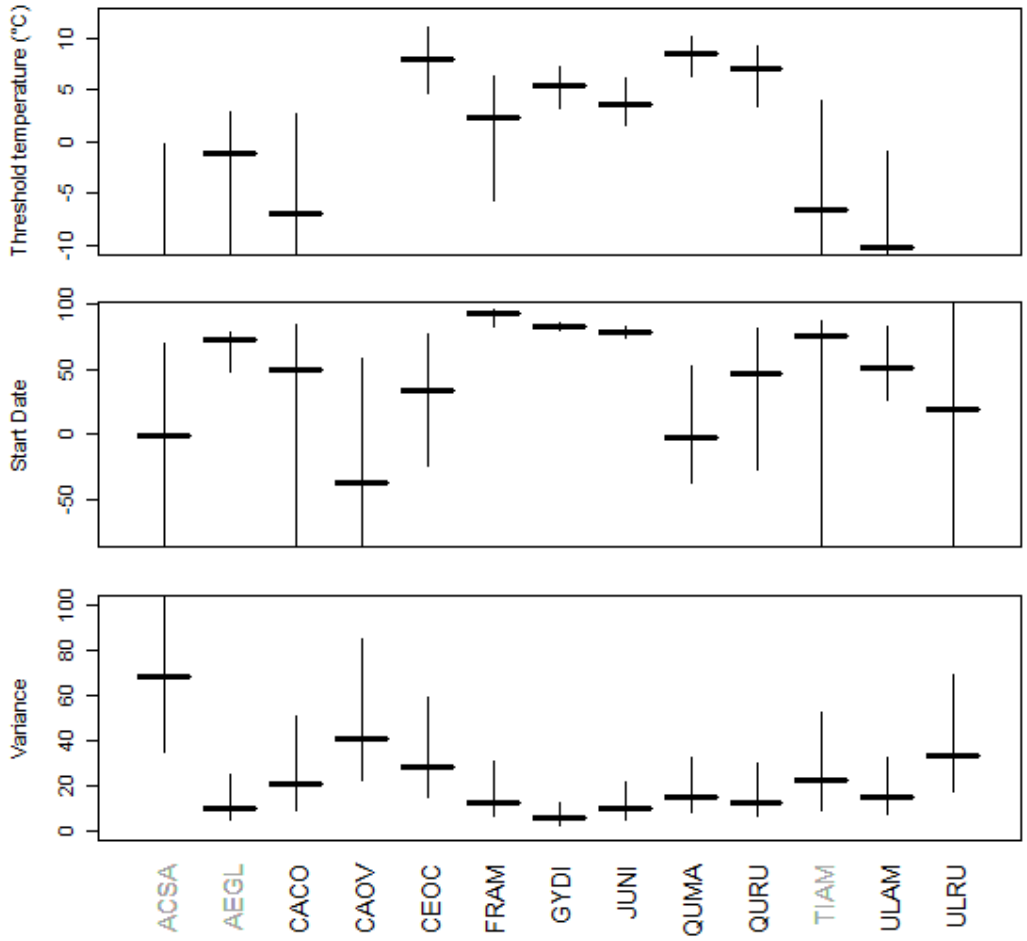

Figure 10. Median parameter estimates (horizontal bars) and 95% credible intervals (vertical bars) for posterior distributions of parameters under the SW model. Parameter ranges are truncated for clarity. For species without visible values for the threshold temperature, the entire credible interval falls below the truncation at -11°C. Species with codes written in black have ring-porous wood anatomy. Species with grey codes are diffuse-porous.

Using the 20th century weather dataset, the mean modeled budburst dates for the various species ranged from April 4 (*Aesculus glabra*) to April 24 (*Fraxinus americana*; Figure 11). Consistent with the observational data on these species (Augspurger et al., 2005), *Aesculus* was the earliest species, with buds opening on average 10 days before the next species. The uncertainty around these dates was generally smaller in species with better identified parameters, ranging from 2 to 11 days.

When the temperatures in the weather dataset were increased by 5°C, all species showed a shift to earlier budburst dates. The extent of this shift differed greatly among species, with mean advancement ranging from 4 d (*Carya ovata*) to 26 d (*Quercus macrocarpa*; Figure 11). The differences in budburst shifts among species resulted in *Aesculus glabra* losing its place as the consistent first species to break bud; under the warmer scenario, it had virtually the same mean budburst date (in late March) as *Acer saccharum, Celtis occidentalis* and *Quercus macrocarpa.* The within-species range of budburst dates due to parameter uncertainty increased for most species under the warmer scenario. Some species, particularly those with narrow budburst CIs under the 20th century climate scenario and small changes in budburst date under + 5°C, showed little or no increase in the width of their budburst date CI under the warmer scenario. However, the remaining species added between 5 and 17 days to their budburst uncertainty window, with the CI for *Acer saccharum* expanding to 27 days (Figure 11).

Most species failed to phenologically keep up with rising temperatures. Only *Quercus macrocarpa*, which had the most extreme shift in mean budburst date in response to warming, showed a tiny (.2 °C) decrease in its mean temperature exposure during the two weeks following budburst (Figure 12). Other species showed an increase in post-budburst temperature ranging between .5 and 4 °C.

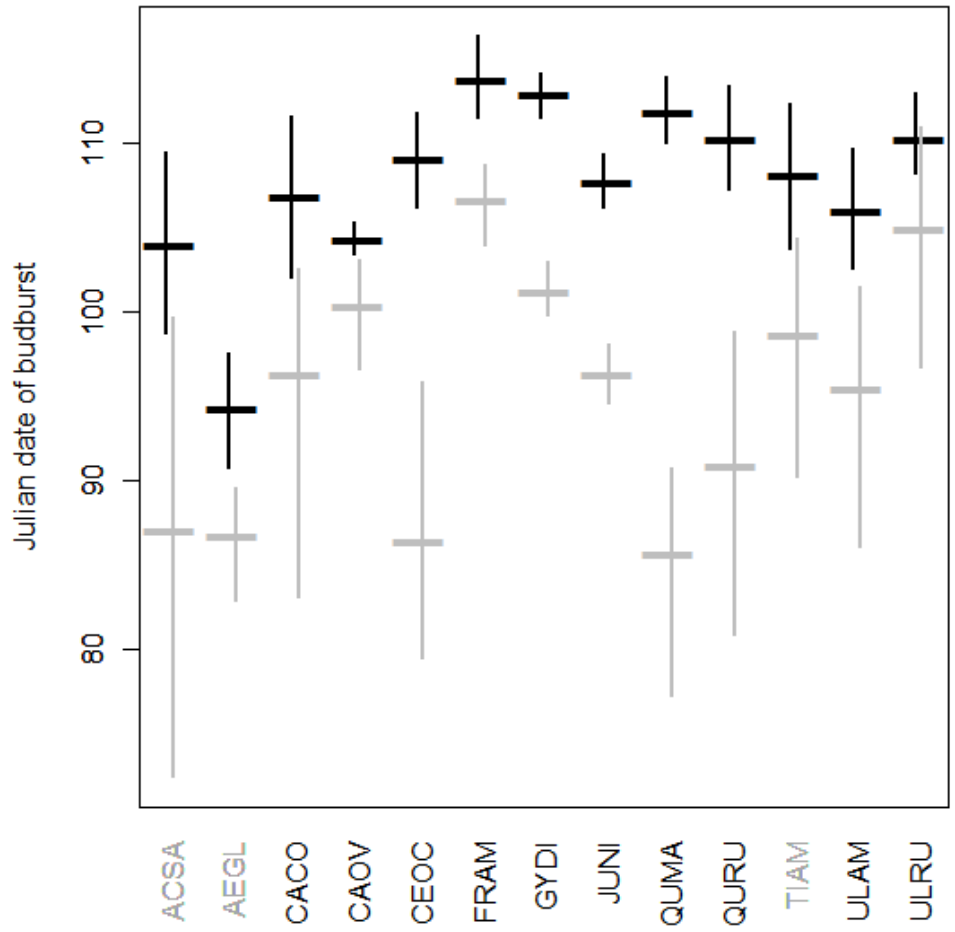

Figure 11. Projected budburst dates for 13 tree species under 20th century and elevated (20th century +5°C) temperatures under the SW model. Horizontal bars show mean budburst dates. The black bars correspond to 20th century climate and the grey bars to the warmer scenario. Vertical lines show the 95% central range of budburst date values associated with model parameter uncertainty. Species codes written in black indicate ring-porous wood. Species with gray codes are diffuse-porous.

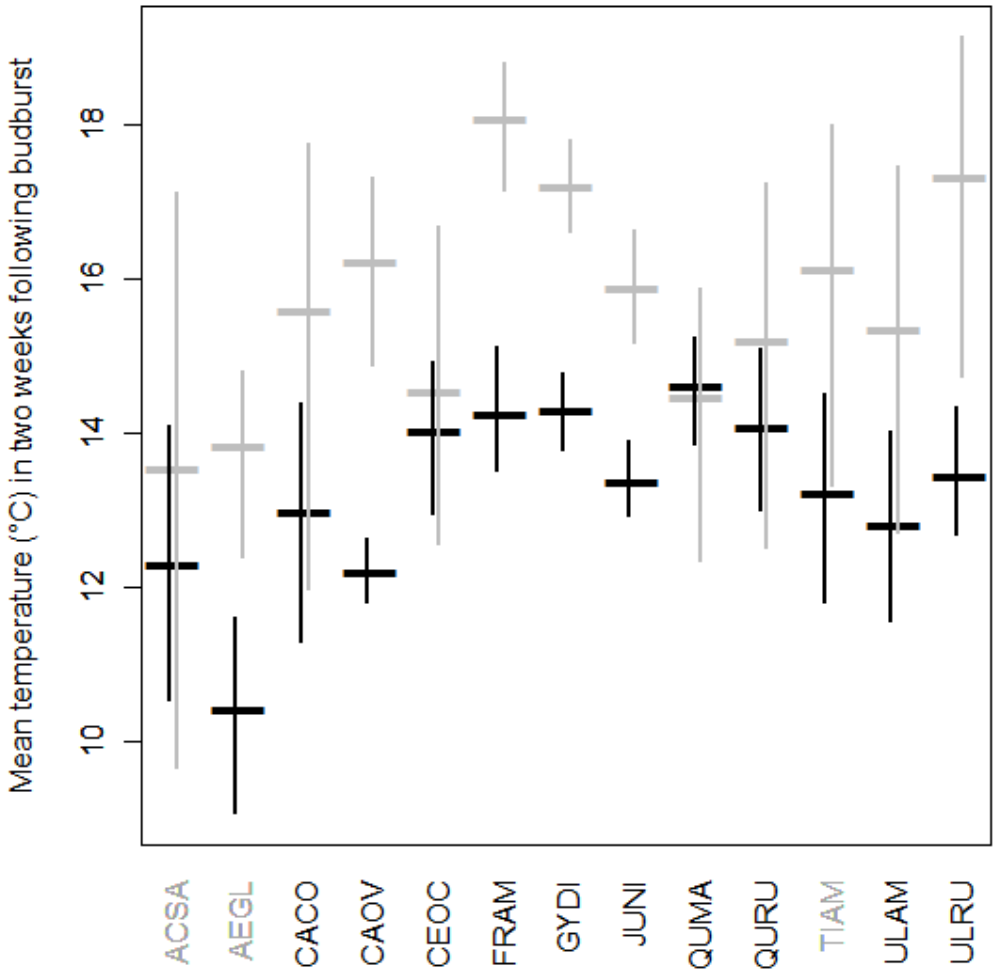

Figure 12. Temperatures during the two weeks following budburst for 13 tree species under 20th century and elevated (20th century +5°C) temperatures under the SW model. The black bars correspond to 20th century climate and the grey bars to the warmer scenario. Horizontal bars show mean post-budburst temperatures, and vertical lines show the 95% central range of post-budburst temperature associated with model parameter uncertainty. Species with codes written in black have ring-porous wood anatomy. Species with grey codes are diffuse-porous.

3.2.2 Chilling-Forcing model

Under the CF model, parameters were generally not well identifiable for most species. The parameter *thresh* was identified within a physiologically reasonable range for *Celtis, Juglans* and the two *Quercus* species, all of which had similar parameter identifiability under the SW model. Other species had unrealistically low values (and wide CIs) for this parameter.

The chilling threshold parameter (*ct*), below which chilling days are counted, had high values for nearly all species. The value of this parameter that is often uncritically accepted in the literature is 5°C (but see Worrall, 1993). Only four out of 13 species

had this value within their 95% central credible intervals (Figure 13). All species had values of this parameter topping out above physiologically (and meteorologically) meaningful ranges. While counting any temperature below 40°C as 'chilling' is clearly ridiculous, such parameter values could still tell us something about the regulation of phenology. When the 'chilling' threshold is very high, every day is counted as a chill day, and this parameter is relegated to simply charting the passage of time, as would be the case if photoperiod was the dominant safety mechanism. It is also important to note that when the value of the parameter *hh* is relatively high, very few chilling days are required to reduce the CF model to essentially the same form as the SW model, so high values of *ct* in this circumstance have no meaning.

The parameter *ff* was generally identified to within a relatively narrow range (Figure 13). This represents the total number of degree-days needed to burst bud when the chilling requirement is essentially satisfied, a quantity that was calculated directly under the SW model. To the extent that variation was seen in this parameter, it was typically trading-off with the *thresh* parameter.

The additional degree-days required to burst bud when no chilling exposure has accrued are represented by the parameter *gg*. This parameter had a very wide CI for nearly all species (Figure 13; note log scale of y-axis for this parameter). However the value of *gg* is largely meaningless when the parameter (*hh*) that mediates decay rate as a function of chilling of is relatively large (i.e. >0.1). This was the case for all but two species, *Carya ovata*, and *Tilia americana*.

While most of these parameters were poorly identified for most species, they still traded off with one another to produce sensible budburst projections (Figure 14). Indeed, the mean values and relative timing of the species differed little from the projections of the SW model, with most species bursting bud on average in late April, except for *Aesculus glabra* which is consistently a few weeks earlier than other species. However, the projections resulting from the CF model generally had wider credible intervals due to parameter uncertainty than those generated with the SW model. As under the SW model, projected budburst dates were much earlier, but also less certain, under the 5°C warming scenario. A similar (but not identical) list of sensitive species virtually caught up with *Aesculus glabra* to form a group of phenologically precocious species (Figure 14). However, no species completely tracked the climate change scenario, with all showing at least a slight increase in the average temperature following budburst (Figure 15).

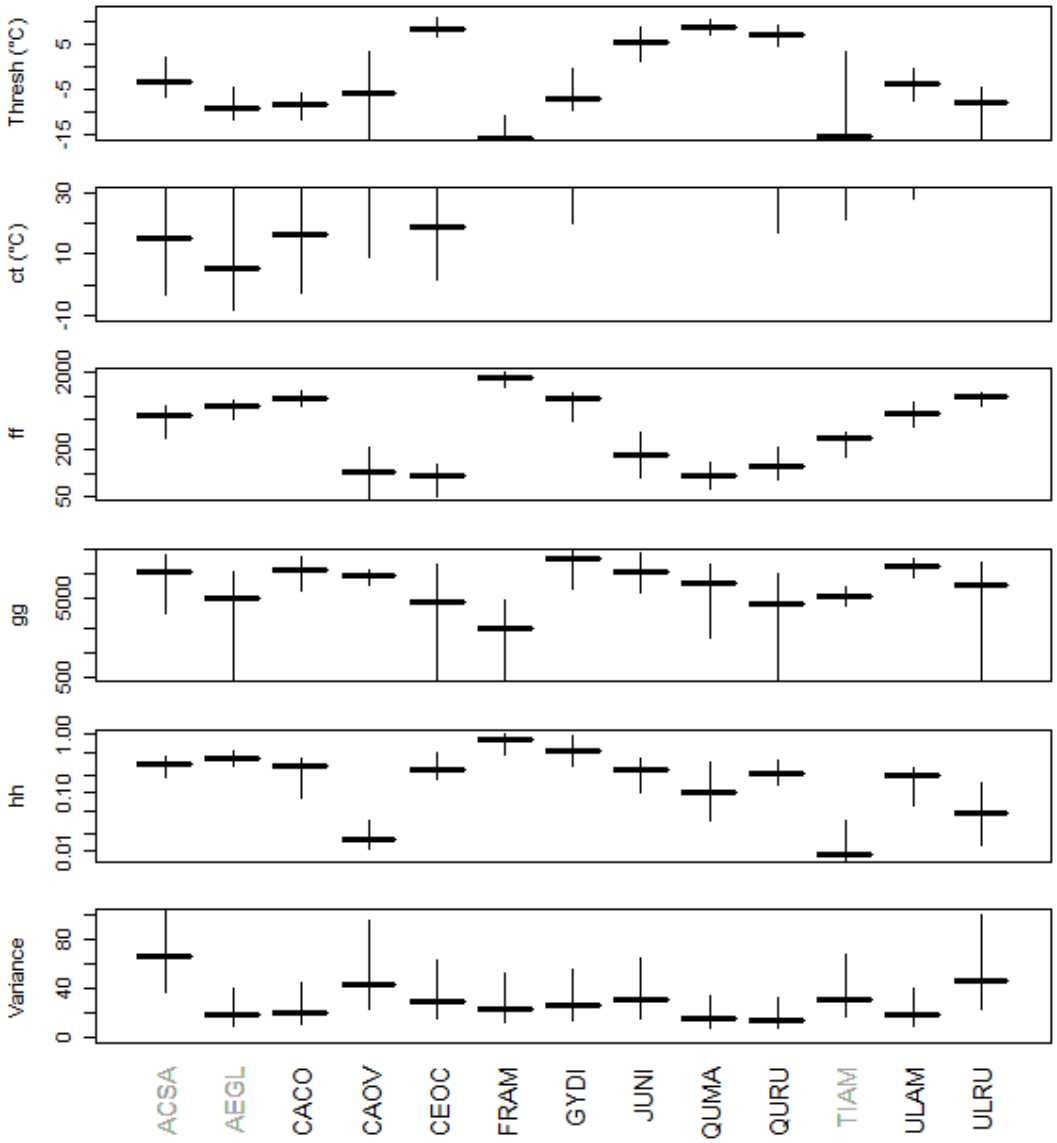

Figure 13. Median parameter estimates (horizontal bars) and 95% credible intervals (vertical bars) for posterior distributions of parameters under the CF model. Parameter ranges are truncated and ff, gg, and hh are plotted on a log scale for clarity. For species with no visible values for the chilling threshold (ct), the entire credible interval falls above the truncation at 31°C. Species with codes written in black have ring-porous wood anatomy. Species with grey codes are diffuse-porous.

3.3 Comparison of fits by model type

While the preceding sections have shown that parameters can be quite difficult to identify under standard budburst models, it is still of interest to compare the basic fits of the models as would be done in a typical phenological study. Typically the selected set of parameters is the one with the 'best' fit, which can be defined in many ways. Here, I

selected the set of parameters with the lowest RMS error between observed and predicted budburst dates from among the 1,000 retained sets of parameters for each species under each model type. As a point of comparison, I also show a null model ('photoperiod') under which budburst is assumed to happen on the same date each year. The SW model was able to improve over the photoperiod model in all cases, particularly for species that had high variability among years (Table 2). The CF model was sometimes a slight improvement over the SW model, but it typically had a worse fit, and occasionally had a slightly worse fit than even the null model.

Table 3. Minimum root-mean-square (RMS) error of observed vs. predicted budburst dates under different model types. The numbers for the SW and CF model represent the lowest error rate (i.e. best fit) of the 1,000 sets of parameters in each species' MCMC chain from the previous sections. The 'Photoperiod' model assumes that budburst happens on the same day every year.

	RMS error (days) by model type		
Species	CF	SW	Photoperiod
ACSAc	7.7	7	9.8
AEGLc	3.4	2.7	5.6
CACOc	4.2	3.6	5.7
CAOVc	6.3	6	6.2
CEOCc	4.6	4.7	9.4
FRAMc	4.5	3.2	5.8
GYDIc	4	2.2	6.4
JUNIc	4	2.8	7.1
QUMAc	3.6	3.6	9.2
QURUc	2.8	3	7.4
TIAMc	5.3	3.6	5.7
ULAMc	3.6	3.4	5
ULRUc	6.3	5.3	5.7

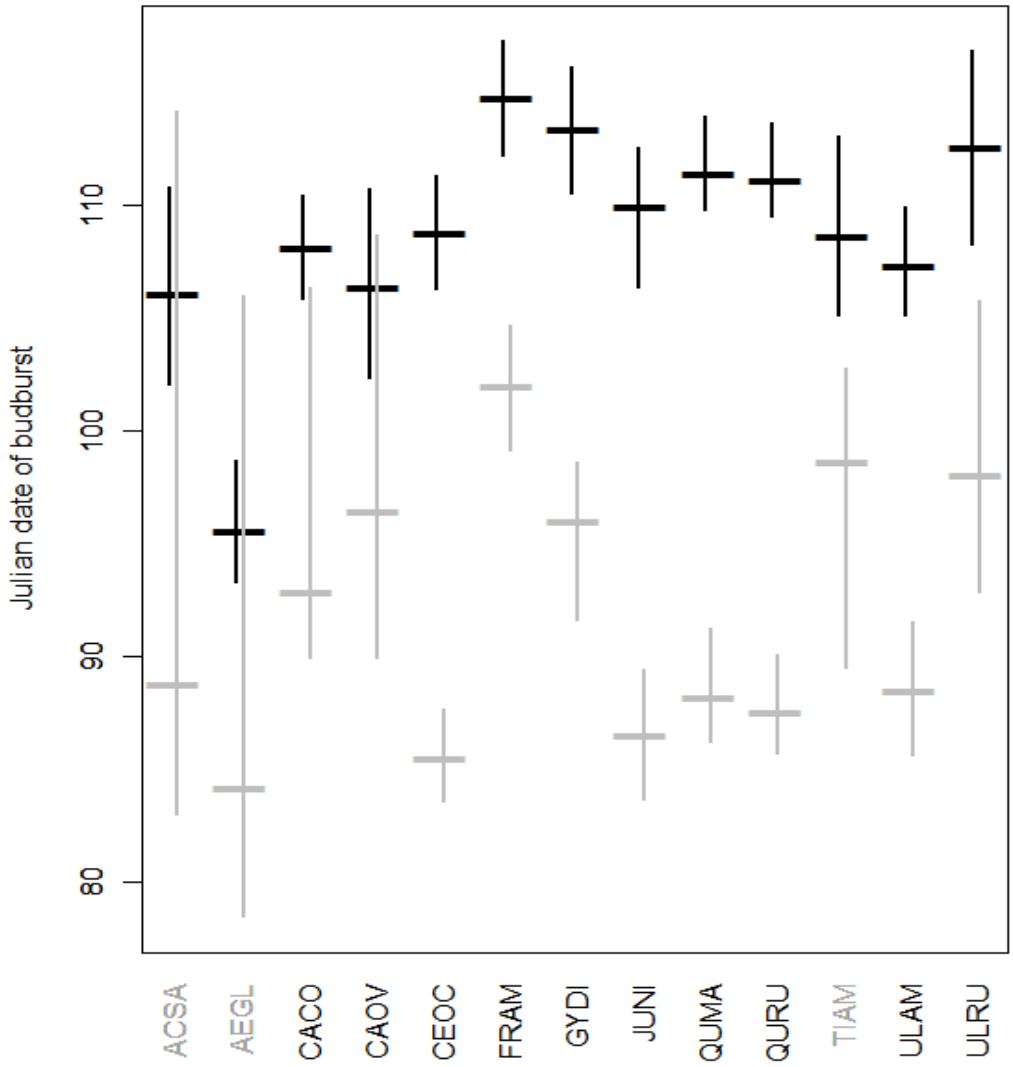

Figure 14. Projected budburst dates for 13 tree species under 20th century and elevated (20th century +5°C) temperatures under the CF model. Horizontal bars show mean budburst dates. The black bars correspond to 20th century climate and the grey bars to the warmer scenario. Vertical lines show the 95% central range of budburst date values associated with model parameter uncertainty. Species with codes written in black have ring-porous wood anatomy. Species with grey codes are diffuse-porous.

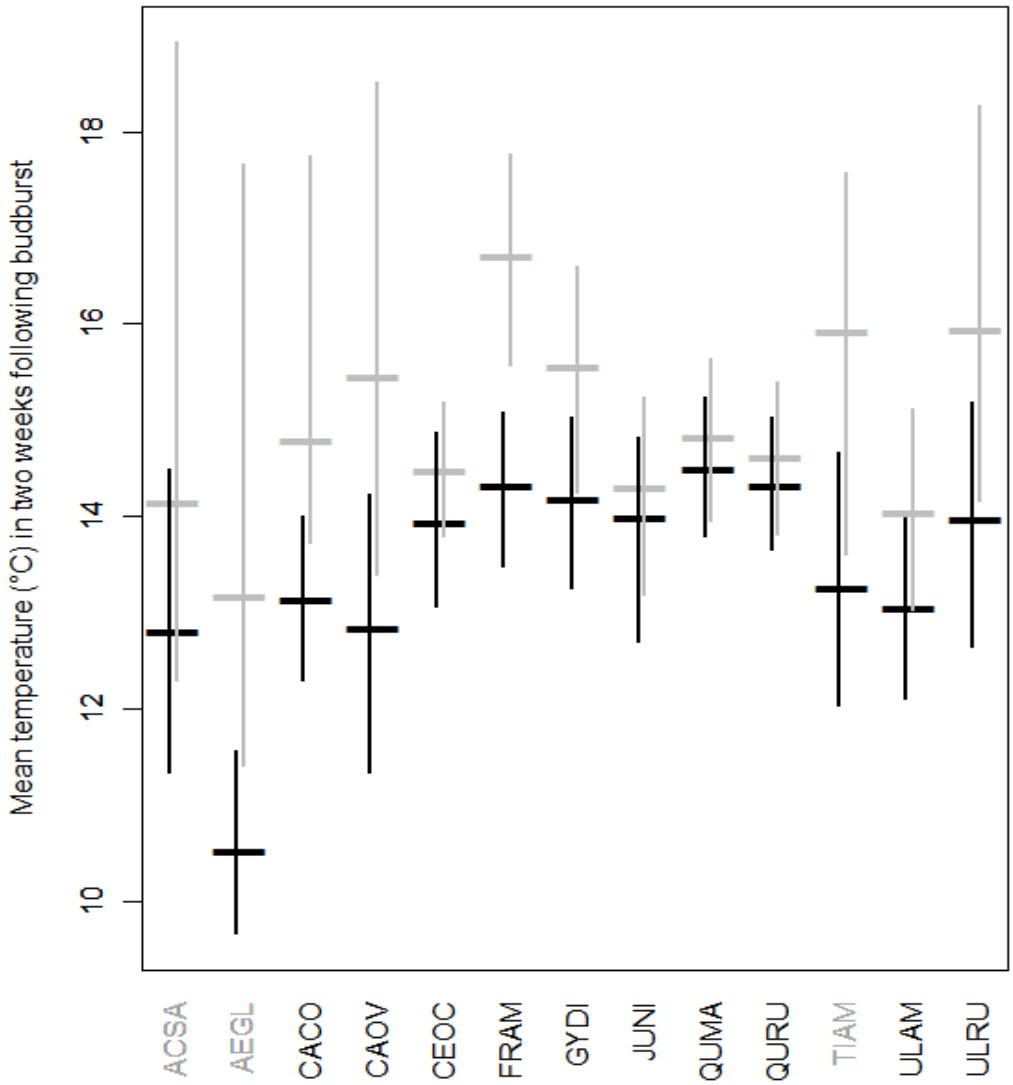

Figure 15. Temperatures during the two weeks following budburst for 13 tree species under 20th century and elevated (20th century +5°C) temperatures under the CF model. The black bars correspond to 20th century climate and the grey bars to the warmer scenario. Horizontal bars show mean post-budburst temperatures, and vertical lines show the 95% central range of post-budburst temperature associated with model parameter uncertainty. Species with codes written in black have ring-porous wood anatomy. Species with grey codes are diffuse-porous.

3.4 Uncertainty of overall growing season length

Under typical central Illinois conditions, leaf senescence begins on 8 October for an average forest tree (C.K. Augspurger, unpublished data). This date is used here as a basis for calculating relative changes in growing season length under the budburst scenarios discussed in the previous section.

For the SW model, warming by 5°C hastened mean budburst dates between 4 and 26 days, depending on species. This is equivalent to a 2.2% to 15.6% increase in growing season length. The 95% credible interval around these dates due to parameter uncertainty ranged from 1.1% to 5.9% of the growing season under 20th century conditions, and from 1.8% to 13.1% under the 5°C warmer scenario.

Among species, the projected mean hastening of budburst with 5°C warming under the CF model ranged from 10 to 23 days. This amounts to an increase of between 6% and 14% in the amount of time trees have for photosynthesis during a growing season. Under the 20th century climate scenario, species' parameter-derived CI width ranged from 2.4% to 5.0% of the growing season. Under the increased temperature scenario, this uncertainty became much larger, ranging up to 15.7% of the growing season for *Acer saccharum*.

4 Discussion

This report has presented a case study of uncertainty in temperate tree function under climate change. It has addressed the overlooked problem of uncertainty in phenological models' parameter estimates, and shown that this problem can be substantial, even when relatively long (18 years) datasets are available. The relationship between parameter uncertainty and precision of projected budburst dates is complex, but the clear message is that parameter uncertainty does matter.

The inability of the more complex CF model to improve over the SW or even in some cases the null 'photoperiod' model suggests it is of very limited use in projecting future budburst dates. While no formal model selection was attempted here, it is clear that the CF model would fail almost any selection criterion. There may be several (non-exclusive) reasons for this failure. The first is the extreme difficulty of exploring high-dimensional parameter spaces. However, longer MCMC runs attempted on some species showed qualitatively similar lack of parameter identifiability under the CF model (results not shown). Another is that the exact form of the CF model may be physiologically incorrect. In any case, such budburst models struggle with some of the same difficulties that would result from simple extrapolation of current budburst trends: namely, the danger of extrapolating beyond the range of available data.

Ultimately, uncertainty in growing season length as projected here is substantial enough to affect the overall carbon balance of the terrestrial biosphere. This report, and all other credible reports of which I am aware, suggest that tree growing seasons will lengthen in a warmer climate. Thus, temperate forests will certainly have more time available for CO_2 uptake. However, the level of uncertainty in these projections limits the extent to which longer growing seasons can be relied upon under carbon accounting schemes. Because the goal of atmospheric greenhouse gas management is to make the probability of some level of warming very small, calculations cannot be based on mean or median values, but rather an extreme quantile corresponding to acceptably small risk values (Lieberman et al., 2007). In the case of a small variance and narrow credible interval, extreme quantiles do not matter so much. When uncertainty is higher, as observed here, extreme values cannot be ignored.

The dramatic shift to earlier budburst with warmer temperatures was unexpected in ring porous species given the sensitivity of their water transport system to frost-induced dysfunction. This brings up the counterintuitive possibility that frost risk may increase

with global warming, particularly if weather fluctuations become more extreme, as is predicted by some models (IPCC, 2007). Increased frost damage due to poorly timed leaf growth may erase any photosynthetic gains due to longer growing seasons (Augspurger, 2009). These possibilities, and the projective uncertainties demonstrated by this research, highlight the need for basic mechanistic understanding of budburst physiology in trees.

While species-level uncertainties in growing season length mostly below 10% may seem small, they could have a disproportionate influence on the carbon balance of forests. A recent study has found that a 20% phenological difference in growing season length corresponded with about a 50% change in annual net ecosystem productivity in a forest in Indiana (Dragoni et al., 2011). While the mechanism for this relationship was not explored, it could be that trees need a certain percentage of the growing season just to 'break even' in terms of productivity, as is seen in alpine plants (Körner, 1999). Thus, the uncertainties reported in this study could have disproportionate impacts on tree and forest productivity.

Climate change can perturb forest carbon balance in many ways. The basic physiology of trees is sensitive to temperature. Many biochemical processes underlying photosynthesis are faster under warmer temperatures (Way and Oren, 2010). However, this benefit may be neutralized by quick re-acclimation of photosynthesis to ambient temperatures (Gunderson et al., 2010). Respiration, or the physiological re-conversion of photosynthates to CO_2, can also reverse carbon gains from various sources. The conventional view of respiration is that it doubles with every 10 °C increase in temperature, posing obvious problems in a warmer climate. However, recent studies have shown that trees down-regulate respiration in the face of warmer temperatures on the scale of a few days (e.g. Lee et al., 2005). Complete local destruction of forests can be caused by fire or insect outbreaks, both of which may be exacerbated by warmer weather (Kurz et al., 2008; Westerling et al., 2006). Extreme weather can have similar impacts. Carbon released from trees damaged and killed by Hurricane Katrina is estimated to be equivalent to a year of CO_2 fixation for all forested areas of the United States (Chambers et al., 2007). This research has added uncertainty in growing season length to this list.

5 References

Augspurger CK, Bartlett EA. Differences in leaf phenology between juvenile and adult trees in a temperate deciduous forest. Tree Physiology 2003; 23:517-525.

Augspurger CK, Cheeseman JM, Salk CF. Light gains and physiological capacity of understorey woody plants during phenological avoidance of canopy shade. Functional Ecology 2005; 19:537-546.

Augspurger CK. Spring 2007 warmth and frost: phenology, damage and refoliation in a temperate deciduous forest. Functional Ecology 2009; 23: 1031-1039.

Cannell MGR, Smith RI. Thermal Time, Chill Days and Prediction of Budburst in *Picea sitchensis*. Journal of Applied Ecology 1983; 20:951-963.

Chambers et al. Hurricane Katrina's carbon footprint on US gulf coast forests. Science 2007; 318:1107.

Chuine I. A unified model for budburst of trees. Journal of Theoretical Biology 2000; 207:337-347.

Clark JS. Models for ecological data. Princeton University Press 2006.

Dragoni D, Schmid HP, Wayson CA, Potter H, Grimmond CSB, Randolph JC. Evidence of increased net ecosystem productivity associated with a longer vegetated season in a deciduous forest in south-central Indiana, USA. Global Change Biology 2011; 17:886-897.

Galik CS, Jackson RB. Risks to forest carbon offset projects in a changing climate. Forest Ecology and Management 2009; 257:2209-2216.

Gunderson CA, KH O'Hara, CM Campion, AV Walker, NT Edwards. Thermal plasticity of photosynthesis: the role of acclimation in forest responses to a warming climate. Global Change Biology 2010; 16(8): 2272-2286.

Harrington RA, Brown BJ, Reich PB. Ecophysiology of exotic and native shrubs in southern Wisconsin .1. Relationship of leaf characteristics, resource availability, and phenology to seasonal patterns of carbon gain. Oecologia 1989; 80:356-367.

Howard WL. An experimental study of the rest period in plants. University of Missouri Agricultural Experiment Station research bulletin 1910; 1.

Hunter AF and Lechowicz MJ. Predicting the timing of budburst in temperate trees. Journal of Applied Ecology 1992; 29:597-604.

IPCC. Contribution of Working Group I to the Fourth Assessment Report of the Intergovernmental Panel on Climate Change, 2007. Solomon, S., D Qin, M Manning, Z Chen, M Marquis, KB Averyt, M Tignor and HL Miller (eds.). Cambridge University Press, Cambridge, United Kingdom and New York, NY, USA; 2007.

Jolly WM, Nemani R, Running SW. A generalized, bioclimatic index to predict foliar phenology in response to climate. Global Change Biology 2005; 11:619-632.

Körner C. Alpine plant life: Functional plant ecology of high mountain ecosystems. Springer, Berlin 1999.

Kurz WA et al. Mountain pine beetle and forest carbon feedback to climate change. Nature 2008; 452:987-990.

Lee TD, PB Reich and PV Bolstad. Acclimation of leaf respiration to temperature is rapid and related to specific leaf area, soluble sugars and leaf nitrogen across three temperate deciduous tree species. Functional Ecology 2005; 19:640-647.

LeQuéré, C, MR Raupach, JG Canadell, G Marland et al. Trends in the sources and sinks of carbon dioxide. Nature Geoscience 2009; 2:831-836.

Liberman, D, M Jonas, Z Nahorski, S Nilsson Eds. Accounting for Climate Change Uncertainty in Greenhouse Gas Inventories - Verification, Compliance, and Trading. Springer 2007.

Menzel A, et al. European phenological response to climate change matches the warming pattern. Global Change Biology 2006; 12:1969-1976.

Metropolis N, Rowenbluth A, Rosenbluth M, Teller A, Teller E. Equation of State Calculations by Fast Computing Machines. Journal of Chemical Physics 1953; 21:1087-1092.

Migliavacca M, E Cremonese, R Colombo, L Busetto, M Galvagno, L Ganis, M Meroni, E Pari, M Rossini, C Siniscalco, U Morra di Cella. European larch phenology in the Alps: can we grasp the role of ecological factors by combining field observations and inverse modelling? International Journal of Biometeorology 2008; 52:587-605.

Morin X, C Augspurger and I Chuine. Process-based modeling of species' distributions: What limits temperate tree species' range boundaries? Ecology 2007; 88:2280–2291.

Morin X, Lechowicz MJ, Augspurger C, O' Keefe J, Viner D, Chuine. Leaf phenology in 22 North American tree species during the 21st century. Global Change Biology 2005; 15:961-975.

Myking T. Effects of constant and fluctuating temperature on time to budburst in *Betula pubescens* and its relation to bud respiration. Trees-Structure And Function 1997; 12:107-112.

Parmesan C, Yohe G. A globally coherent fingerprint of climate change impacts across natural systems. Nature 2003; 421:37-42.

Peñuelas J, Rutishauser T, Filella I. Phenology Feedbacks on Climate Change. Science 2009; 324:887-888.

Perkey AW, Wilkins BL and Smith, HC. Crop tree management in eastern hardwoods. USDA Forest Service publication NA-TP-19-93. 1994.

Picard G, Quegan S, Delbart N, Lomas MR, Le Toan T, Woodward FI. Bud-burst modelling in Siberia and its impact on quantifying the carbon budget. Global Change Biology 2005; 11:2164-2176.

Réaumur RAFd. Observations du thermomètre, faites a Paris pendant l'année 1735, comparées avec celles qui ont été faites sous la ligne, à l'isle de France, à Alger et quelques unes de nos isles de l'Amérique. Memoires de l'Académie des Sciences de Paris 1735; 545-376.

Sarvas R. Investigations on the annual cycle of development of forest trees. II. Autumn dormancy and winter dormancy. Communicationes Instuti Forestalis Fenniae 1974; 84:1-101.

Stevens, PF. Angiosperm Phylogeny Website. Version 9, June 2008. http://www.mobot.org/MOBOT/research/APweb/; 2001 onwards.

Tyree MT and MH Zimmerman. Xylem structure and the ascent of sap. Springer; 2002.

Way DA and R Oren. Differential responses to changes in growth temperature between trees from different functional groups and biomes: a review and synthesis of data. Tree Physiology 2010; 30(6):669-688.

Westerling et al. Warming and earlier spring increase western US forest wildfire activity. Science 2006; 313:940-943.

Worrall J. Temperature effects on bud-burst and leaf-fall in subalpine larch. Journal of Sustainable Forestry 1993; 1:1-18.

Appendix – Clarifying tables on models and abbreviations

Table A1. Acronyms, symbols, abbreviations, and parameters used in this report.

Abbreviation	Meaning	Units
σ	Error term variance from both the CF and SW models.	$days^2$
BB	Budburst (date) – the date on which leaf tissue emerges from opening buds.	days (Julian)
BBE	Expected budburst date	days (Julian)
BBO	Observed budburst date	days (Julian)
CD	Chill days – the observed number of days with mean temperature below *ct*	days
CF	Chilling-forcing model – the more complex of the two models investigated in this report.	NA
ct	Chilling threshold – a parameter that mediates the mean daily temperature below which chill days (CD) accumulate in the CF model.	°C
DD	Degree-days – The time-integrated exposure to temperatures above the threshold '*thresh*'	°C·days
DD*	Critical DD sum – The accumulated number of degree days required to induce budburst.	°C·days
ff	A parameter mediating the tradeoff between chilling and warmth exposure in the CF model. This parameter can be thought of as the minimum number of degree-days to which a tree must be exposed in order to break bud when the chilling requirement is well satisfied.	°C·days
gg	A parameter mediating the tradeoff between chilling and warmth exposure in the CF model. This parameter can be thought of as the additional number of degree days above *ff* required to cause budburst when a tree has been exposed to no chilling.	°C·days
hh	A parameter mediating the tradeoff between chilling and warmth exposure in the CF model. This parameter can be thought of as the steepness with which the degree-day requirement decreases with each additional day of chilling.	$days^{-1}$
$I_{d,y}$	An indicator that is equal to one if the daily mean temperature on day *d* in year *y* is greater than *thresh* and equal to zero otherwise.	unitless
IPCC	Intergovernmental Panel on Climate Change	NA
$L_{d,y}$	An indicator that is equal to one if the daily mean temperature on day *d* in year *y* is less than c*t* and equal to zero otherwise.	
MCMC	Markov-chain Monte Carlo	NA
RMS	Root mean square	NA
startdate	The date after which DD accumulation begins.	days (Julian)
SW	Spring warming model – the simpler of the two models investigated in this report.	NA
$T_{d,y}$	Mean daily temperature on day *d* in year *y*.	°C
t	Date	Days
thresh	Temperature threshold above which degree days are accumulated	°C

Table A2. A summary of the parameters included in each model and the numerical values which they may take.

Model	Parameter	Units	Parameter range
Spring Warming (SW)	*startdate*	days (Julian)	Lower bound: September 1st of the previous year; no upper bound imposed in the MCMC routine
	thresh	°C	No limits imposed in MCMC routine
	σ	$days^2$	All positive numbers allowed
Chilling-Forcing (CF)	*thresh*	°C	No limits imposed in MCMC routine
	ct	°C	No limits imposed in MCMC routine
	ff	°C·days	All positive numbers allowed
	gg	°C·days	All positive numbers allowed
	hh	$days^{-1}$	All positive numbers allowed
	σ	$days^2$	All positive numbers allowed